

Development of nascent autotrophic carbon fixation systems in various redox conditions of the fluid degassing in early Earth

Sergey A. Marakushev, Ol'ga V. Belonogova

5 Institute of Problems of Chemical Physics, Russian Academy of Sciences, Academician Semenov avenue 1, Chernogolovka, Moscow region, 142432 Russian Federation

Correspondence: Sergey A. Marakushev (shukaram@yandex.ru; marak@cat.icp.ac.ru)

10 **Abstract.** Strategies for the origin and development of primary metabolism on early Earth were determined by the two main regimes of degassing of Earth - reducing and oxidative (methane and CO₂ predominance, respectively). Among the existing theories of the autotrophic origin of the life, CO₂ is usually considered the carbon source for nascent autotrophic metabolism. However, the ancestral carbon used in metabolism may have been
15 derived from CH₄ if the outflow of magma fluid to the surface of the Earth consisted mainly of methane. In an environment with a high partial pressure of methane, primary metabolic systems could arise, the carbon source for which was preferably methane. Due to the absence of molecular oxygen in the Archean conditions, this metabolism would have been anaerobic, i.e., oxidation of methane must be realized by inorganic high-potential electron acceptors. In
20 light of the primacy and prevalence of CH₄-dependent metabolism in hydrothermal systems of the ancient Earth, we propose a model of carbon fixation, which is a sequence of reactions in a hypothetical methane-fumarate cycle. Thermodynamics calculations showed a high efficiency of oxidation of methane to acetate (methanotrophic acetogenesis) by oxidized nitrogen compounds in hydrothermal systems. The hydrothermal system is considered in the
25 form of a phase diagram, which demonstrates the area of redox and P, T conditions favorable for the development of primary methanotrophic metabolism.

1 The deep methane degassing of early Earth

30 Presence of the magnetic fields of planets and satellites is correlated with their endogenous activity in the form of volcanism and fluid flows. The deep hydrocarbon generation on seismically active satellites manifests in the form the significant concentrations of hydrocarbons, including methane, on their surface. For example, there is a prevalence of

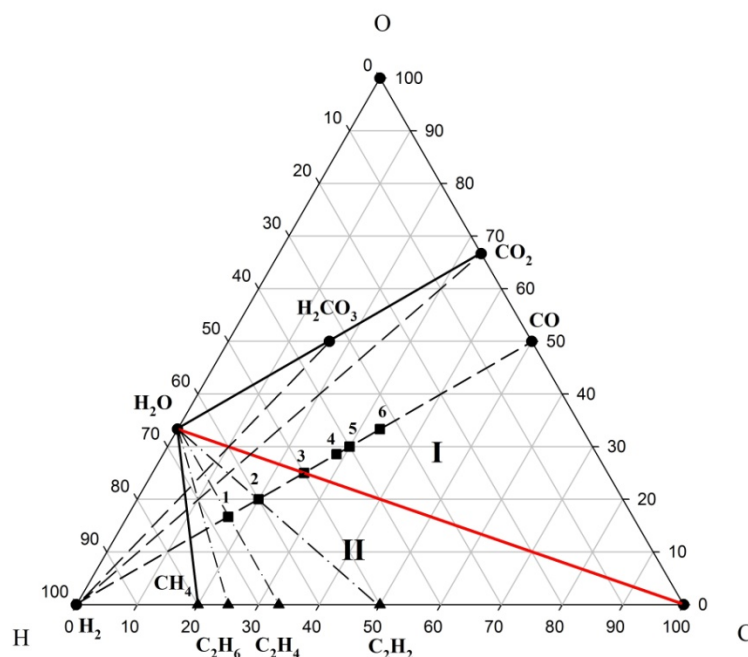
methane on Titan and Enceladus (the satellites of Saturn) (Tobie et al., 2006; Bouquet et al., 2015) and on Europa (the satellite of Jupiter) (e.g. Russell et al., 2017). Additionally, high concentrations of methane are assumed to be present on early Mars (Oehler and Etiope, 2017).

On Earth, the methane and other hydrocarbons are generated in magma chambers and are carried by fluids to the surface in volcanic processes, and during the minerals formation are trapped in the gas-liquid inclusions. This has been observed in the quartz–methane amygdaline inclusions that occur in the form of relics present even in metamorphic-basaltic rocks of Greenland that are aged at 3.8 billion years (Touret, 2003). Inclusion of hydrocarbons and reduced organic compounds in Archean quartz (Touret, 2003, Schreiber et al., 2017) indicates a sufficiently reductive environment at this time. There is evidence that Archean atmosphere was enriched in hydrogen and methane (Tian et al, 2005; Zahnle et al, 2019), but the oxidation state of magma sources apparently has changed (Aulbach et al, 2017.). According the trace-elements data of crustal origin igneous zircons (mainly Ce-based oxybarometer), it was shown that the Hadean continental crust was significantly more reduced than its modern counterpart and experienced progressive oxidation ~3.6 billion years ago (Yang et al., 2014). Regarding quartz - fayalite - magnetite redox buffer, the state of the earth's crust periodically changed from -8 to +4 in Hadean and from -7 to +7 in the early Archean. Significant fluctuations in the redox state of Archean and Hadean zircons indicate a pulsed regime of earth degassing during this period of time, which, in our opinion, is related to impulses in the geomagnetic field (Allredge, 1984; Larson and Olson, 1991; Aubert et al., 2010). Thus, the evolution of the Earth over a period of 4.6 billion years is determined by the impulsive degassing of its liquid core along the structures of the dislocation of its solid silicate shells (mantle and crust).

Of all the magmatic formations of the world the alkaline magmatism is the deepest, and in its magma chambers hydrocarbon substances arises. Thermodynamic calculations show the preference of deep formation and stability of hydrocarbons, which, rising in fluids to the surface of the Earth (temperature and pressure decreasing), are transformed to methane (Marakushev and Marakushev, 2006). This is confirmed by the massive production of abiogenic methane at ~40 km depth (Brovarone et al., 2017) and the discovered bubbles of hydrocarbons trapped in eclogite, a metamorphic rock that forms at high pressure at a depth of at least 80 km (Tao et al., 2018). The gas-liquid inclusions of methane in diamond, and P,T experiments on the synthesis of hydrocarbons (Smit et al., 2016) also prove its deep origin. The global mid-ocean ridge system represents a major site for outgassing of volatiles from

Earth's mantle. Methane, which was considered to be of relative surface origin (low-temperature serpentinization $\sim 100^\circ\text{C}$), apparently to be deep, forming at temperatures at ca. 400 $^\circ\text{C}$ under redox conditions characterizing intrusive rocks derived from sub-ridge melts (Mével, 2003; Wang et al., 2018). Thus, deep, alkaline - basalt magmatism (elevated alkali content, especially K_2O), in contrast to basalt-andesitic one, is mainly responsible for methane degassing on the Earth's surface. With increasing alkalinity (alkaline slope) in the fluid inclusions of igneous minerals invariably appear different hydrocarbons (Potter and Konnerup-Madsen, 2003; Nivin et al., 2005). The high content of potassium in the high-silica Hadean crust (Boehnke et al., 2018) indicates the depth of magmatism and its hydrocarbon specificity.

Fluids ejected from the liquid core were initially saturated with hydrogen, with oxygenic components being of minor importance. However, when the permeability of silicate shells across the Earth increased (during the expansion of silicate shells of the Earth due to the oscillatory nature of the geomagnetic field), there began a selective migration of hydrogen, the most mobile component, out of the fluid. This process is responsible for hydrogen losing its leading position in ejected fluids and being fundamental to the evolution of low and normal alkalinity magmatism (Marakushev and Marakushev, 2008, 2010). In this scenario, the fractionation of chemical components in fluid would result in rich acidic CO_2 solutions (for example, $\text{H}_2 + 2\text{CO} = \text{H}_2\text{O} + 0.5\text{CO}_2 + 1.5\text{C}$ and $\text{H}_2\text{O} + \text{CO}_2 = \text{H}_2\text{CO}_3$). These solutions are widely observed in the composition of fluid inclusions in minerals of all igneous rocks of low and normal alkalinity. In Fig. 1, this region of thermodynamic stability (facies) representing the paragenetic association of $\text{H}_2\text{O}-\text{C}-\text{CO}_2$ is denoted by **(I)**.



90

Figure 1. Two regimes of evolution of the C–H–O system on the phase diagram of its compositions. Roman numerals denote various regimes of hydrogen fluid evolution: **(I)** water-carbonic and **(II)** water-hydrocarbon solutions, separated by H₂O–C equilibrium (red). Parageneses (assemblages) of the initial substances (H₂, CO, CO₂) are denoted by dashed sub-
 95 lines, while dash-dotted lines indicate the parageneses (C₂H₆–H₂O, C₂H₄–H₂O, etc) of hydrocarbons (black triangles) with water. Black squares denote organic substances within the two component (H₂–CO) subsystem: m ethanol (1), ethylene glycol (2), acetate (3), succinate (4), pyruvate (5), and fumarate (6).

100 The transition to compression of silicate shells prevents hydrogen migration from fluids and stimulates the production of hydrocarbons within them; for example, consider the reactions: $3\text{H}_2 + \text{CO} = \text{H}_2\text{O} + \text{CH}_4$, $5\text{H}_2 + 2\text{CO} = 2\text{H}_2\text{O} + \text{C}_2\text{H}_6$ (Fig.1, facies **II**, reducing conditions). The hydrogen in the reaction like $4\text{H}_2 + \text{H}_2\text{CO}_3 = 3\text{H}_2\text{O} + \text{CH}_4$ destroys the acid components in fluids, and this determines the alkaline slope in the development of
 105 magmatism. This is a two-stage model of the development of the C–H–O system (**I** ↔ **II**), which depends on the composition of Earth's core fluids, and their transformations in magma chambers.

The existing theories on the origin of autotrophic life identify carbon dioxide as the unique carbon source for metabolism. This autotrophic metabolism should have originated at
 110 a high partial pressure of CO₂ in the environment (paragenesis CO₂ + H₂O, Fig. 1, facies **I**). We assume that in geodynamic regime **II** (CH₄ + H₂O paragenesis), carbon ancestral

metabolism could use methane as a carbon source if the flow of free energy from the geochemical environment was coupled with biomass formation reactions. Perhaps, these different regimes of fluid degassing determined the physicochemical conditions of ambient environment, which, in turn, provided an opportunity of emergence and development of various systems of ancient autotrophic metabolism. In regime II (Fig. 1), carbon fixation could occur in the form of methane or other hydrocarbons.

The above geochemical and petrological data indicate highly heterogeneous redox conditions between the present-day Earth and conditions that periodically arose in the early Earth. We consider that the anaerobic reductive geochemical conditions of the Archean played a decisive role in the origin and development of carbon and energy metabolism, which were vastly different from those observed in the tops of the branches of the modern phylogenetic tree of prokaryotes. Most metabolically-anaerobic chemoautotrophic organisms are either extinct or strongly limited to narrow anoxic ecological niches. Lateral gene transfer and subsequent phylogenetic divergence erased most evolutionary information recorded in ancestral prokaryotic genomes (Martin et al., 2016).

2 Anaerobic oxidation of methane

The study of anaerobic oxidation of methane (AOM) in modern oxygen-free environments (marine sedimentary rocks, gas-hydrates, mud volcanoes, black smokers, hydrocarbon seeps) has increased in recent years. This direction was sparked by the discovery of anaerobic methanotrophic archaea (Hinrichs et al., 1999) and, subsequently, their structural consortia with sulfate-reducing bacteria (Knittel and Boetius, 2009). A similar relationship was later discovered in archaea species that functions in chemical conjunction with the bacterium *Candidatus Methyloirabilis oxyfera*, which itself can independently couple AOM to denitrification (Ettwig et al., 2010; Haroon et al 2013). Furthermore, the microbiological AOM was recently shown to be directly associated with the reduction of iron and manganese compounds and minerals (Beal, 2009; Ettwig et al., 2016; Oni and Friedrich, 2017; He et al., 2018), as, for example, in the reaction $\text{CH}_4 + 8\text{Fe}^{3+} + 2\text{H}_2\text{O} \rightarrow \text{CO}_2 + 8\text{Fe}^{2+} + 8\text{H}^+$ ($\Delta G^{0'} = -454 \text{ kJ mol}^{-1} \text{ CH}_4$).

Recent studies have suggested that both archaea (ANME-2d) (Haroon et al., 2013) and bacteria (*Methylobacter*) (Martinez-Cruz et al., 2017), without partners, may themselves be versatile methanotrophs capable of using different oxidants as electron acceptors under different environmental conditions. AOM is proposed to occur by reversal of the canonical

methanogenesis pathway. For example, nickel enzyme purified from methanogenic archaea can catalyze the oxidation of methane to methyl coenzyme M ($\text{CH}_4 + \text{CoM-S-S-CoB} \rightarrow \text{CH}_3\text{-S-CoM} + \text{HS-CoB}$; $\Delta G^\circ = 30 \pm 10 \text{ kJmol}^{-1}$), that is the reverse reaction of methyl coenzyme M reductase (Scheller et al., 2010). In general, methano- and methylotrophs use
150 different but often interrelated pathways of carbon fixation (Smejkalová et al., 2010). Newly described methanotrophic anaerobic prokaryotes are frequently discovered in various extreme environmental conditions (Semrau et al., 2008), underscoring the functional and phylogenetic diversity of this group. The search for relict forms of anaerobic methanotrophic metabolism continues.

155 In 2013, Wolfgang Nitschke and Michael Russell described the possibility of methane assimilation as the sole source of carbon for primordial metabolism (Nitschke and Russell, 2013). They suggested that methanotrophy and not methanogenesis may have been the founding metabolism in the first protocells and presented a model of methanotrophic acetogenesis in which methane, as the carbon source, is assimilated into the biomimetic
160 analogue of the modern reverse acetyl-CoA pathway. The proposed methane oxidant in this pathway of CH_4 fixation was activated nitric oxide (NO), formed via nitrate/nitrite transformation ('denitrifying methanotrophic acetogenesis') (Russell and Nitschke, 2017). The authors consider the process of low-temperature harzburgite (ophiolites) hydrothermal serpentinization in the presence of carbon oxides served as the main source of methane.
165 Nevertheless, Wang et al. (2018) argue that there is another unified deep high-temperature process of methane making for these hydrothermal areas.

In the absence of oxygen the methane oxidation requires electron acceptors with a high redox potential (such as nitrate, manganese (IV), iron (III), and sulfate). Thermodynamic calculations of anaerobic methanotrophic acetogenesis reactions in aqueous hydrothermal
170 conditions that require oxidized compounds such as sulfur, nitrogen, and iron are considered in Table 1. For example, the free energy of the reaction $\text{CH}_4 + 6\text{Fe}_2\text{O}_3 = 0.5\text{CH}_3\text{COOH} + \text{H}_2\text{O} + 4\text{Fe}_3\text{O}_4$ at 473 K is equal to the sum of the free energy of products formation minus the sum of free energy of the reactants formation at the same temperature ($\Delta G_{473}^0 = (0.5\Delta G_{\text{CH}_3\text{COOH}}^0 + \Delta G_{\text{H}_2\text{O}}^0 + 4\Delta G_{\text{Fe}_3\text{O}_4}^0) - (\Delta G_{\text{CH}_4}^0 + 6\Delta G_{\text{Fe}_2\text{O}_3}^0) = -6.49 \text{ kJ/mol}$).

175

Table 1. Free Gibbs energy of aqueous reactions of anaerobic methanotrophic acetogenesis at 298 and 473 K at the saturated vapor pressure (P_{SAT}). The oxidized and reduced states of oxidant in the reaction are conditionally called the redox pairs. The

oxidation of methane to fully ionized and non-ionized forms of acetate is presented. TR –
 180 represents the temperature regime of the reactions from low (L) to high-temperatures (H).
 Free energies of aqueous substances formation at P_{SAT} (Amend and Shock, 2001) were used
 in calculations.

Redox pair of nitrogen	ΔG^0_{298} kJ/mol CH ₄	ΔG^0_{473} kJ/mol CH ₄	TR
CH ₄ + 2NO = 0.5CH ₃ COOH + H ₂ O + N ₂	-586.78	-563.18	L
CH ₄ + 2NO = 0.5CH ₃ COO ⁻ + 0,5 H ⁺ + H ₂ O + N ₂	-573.39	-538.33	
CH ₄ + 4NO = 0.5CH ₃ COOH + H ₂ O + 2N ₂ O	-582.32	-535.87	L
CH ₄ + 4NO = 0.5CH ₃ COO ⁻ + 0,5 H ⁺ + H ₂ O + 2N ₂ O	-568.93	-511.02	
CH ₄ + 4HNO ₂ = 0.5CH ₃ COOH + 3H ₂ O + 4NO	-264.46	-320.79	H
CH ₄ + 4NO ₂ ⁻ + 3.5H ⁺ = 0.5CH ₃ COO ⁻ + 4NO + 3H ₂ O	-324.71	-398.7	
CH ₄ + 2HNO ₃ = 0.5CH ₃ COOH + H ₂ O + 2HNO ₂	-295.16	-286.35	L
CH ₄ + 2NO ₃ ⁻ = 0.5CH ₃ COO ⁻ + 2NO ₂ ⁻ + H ₂ O + 0.5H ⁺	-230.07	-217.58	
CH ₄ + 1.33HNO ₃ = 0.5CH ₃ COOH + 1.67H ₂ O + 1.33NO	-286.41	-299.38	H
CH ₄ + 1.33NO ₃ ⁻ + 0.83H ⁺ = 0.5CH ₃ COO ⁻ + 1.33NO + 1.67H ₂ O	-263.12	-304.34	
CH ₄ + 0.8HNO ₃ = 0.5CH ₃ COOH + 1.4H ₂ O + 0.4N ₂	-405.67	-403.98	L
CH ₄ + 0.8NO ₃ ⁻ + 0.3H ⁺ = 0.5CH ₃ COO ⁻ + 0.4N ₂ + 1.4H ₂ O	-386.33	-382.11	
Redox pair of iron (mineral buffers)			
CH ₄ + 6Fe ₂ O ₃ = 0.5CH ₃ COOH + H ₂ O + 4Fe ₃ O ₄	11.84	-6.49	H
CH ₄ + 6Fe ₂ O ₃ = 0.5CH ₃ COO ⁻ + 0,5 H ⁺ + H ₂ O + 4Fe ₃ O ₄	25.23	18.36	H
CH ₄ + 1.5FeS ₂ + 0.5Fe ₃ O ₄ = 0.5CH ₃ COOH + H ₂ O + 3FeS	44.65	28.85	H
CH ₄ + 1.5FeS ₂ + 0.5Fe ₃ O ₄ = 0.5CH ₃ COO ⁻ + 0,5 H ⁺ + H ₂ O + 3FeS	58.04	53.7	H
CH ₄ + 2Fe ₃ O ₄ + 3SiO ₂ = 0.5CH ₃ COOH + H ₂ O + 3Fe ₂ SiO ₄	57.23	16.19	H
CH ₄ + 2Fe ₃ O ₄ + 3SiO ₂ = 0.5CH ₃ COO ⁻ + 0,5 H ⁺ + H ₂ O + 3Fe ₂ SiO ₄	70.62	41.04	H
Redox pair of sulphur			
CH ₄ + 0.5H ₂ SO ₄ = 0.5CH ₃ COOH + H ₂ O + 0.5H ₂ S	-42.57	-69.93	H
CH ₄ + 0.5SO ₄ ²⁻ + 0,5 H ⁺ = 0.5CH ₃ COO ⁻ + H ₂ O + 0.5H ₂ S	-29.18	-45.07	
Carboxy-methano acetogenesis			
CH ₄ + CO ₂ + 2NO + 2H ₂ = CH ₃ COOH + N ₂ + 2H ₂ O	-671,53	-620,83	L
CH ₄ + HCO ₃ ⁻ + 2NO + 2H ₂ = CH ₃ COO ⁻ + N ₂ + 3H ₂ O	-680.97	-636.35	
CH ₄ + 0.5CO ₂ + 6Fe ₂ O ₃ + H ₂ = 0.75CH ₃ COOH + 4Fe ₃ O ₄ + 1.5H ₂ O	-30.54	-35.34	H
CH ₄ + 0.5HCO ₃ ⁻ + 6Fe ₂ O ₃ + H ₂ = 0.75CH ₃ COO ⁻ + 4Fe ₃ O ₄ + 2H ₂ O + 0,25H ⁺	-28.56	-30.64	
CH ₄ + CO ₂ = CH ₃ COOH	24.27	39.89	L
CH ₄ + HCO ₃ ⁻ = CH ₃ COO ⁻ + H ₂ O	14.83	24.41	
Carboxy- acetogenesis			
CO ₂ + 2H ₂ = 0,5CH ₃ COOH + H ₂ O	-84,75	-57,65	H
HCO ₃ ⁻ + 2H ₂ + 0,5H ⁺ = 0,5CH ₃ COO ⁻ + 2H ₂ O	-107,58	-98,01	

It is obvious that methane oxidation with nitrogen oxide compounds is
 185 thermodynamically very favorable, compared to oxidants such as sulfate, magnetite and
 hematite. The acetogenesis reactions are energetically more preferable under acidic
 hydrothermal conditions (the protonated compounds). The change in the free energy with
 temperature change indicates whether the reaction displays a thermodynamic preference for
 low-temperature (L) or high-temperature (H) conditions. The reactions of methane with
 190 sulfate and iron-oxides is the most thermodynamically favorable with increasing temperature
 (decreasing ΔG^0_r), whereas the reactions with nitrogen-oxides have different directions. The

methane fixation is an energetically more favorable process than CO₂ fixation. For example, in aerobic acetogenesis (CH₄+O₂ = 0,5CH₃COOH+H₂O), more free energy is released in the methane fixation reaction ($\Delta G^0_{298} = -417.35$ kJ/mol under standard conditions; aqueous constants from (Amend and Shock, 2001)) than in the process of CO₂ fixation (CO₂+2H₂= 0,5CH₃COOH+H₂O; $\Delta G^0_{298} = -84.75$ kJ/mol).

The most favorable reaction CH₄ + 2NO = 0,5CH₃COOH + H₂O + N₂ (Table 1) can be represented as a model of methanotrophic acetogenesis, which is the part of the reverse acetyl-CoA pathway. The second part of this path is the reaction of CO₂ reduction: CO₂ + 2H₂ = 0,5CH₃COOH + H₂O. In sum, this is a very thermodynamically favorable pathway of carbon fixation in the form CH₄ и CO₂: CH₄ + CO₂ + 2NO + 2H₂ = CH₃COOH + N₂ + 2H₂O. Somewhat different stoichiometry of acetogenesis was observed in the Archean Methanosarcina acetivorans, when methane oxidation was associated with the reduction of iron (III) [Soo et al, 2016]. A reaction is proposed in which four methane molecules are oxidized and two CO₂ molecules are reduced to form three acetate molecules. Increasing the ratio of CH₄ to CO₂ (4CH₄ + 2CO₂ + 24Fe₂O₃ + 4H₂ = 3CH₃COOH + 6H₂O + 16Fe₃O₄) makes the process of anaerobic acetogenesis more thermodynamically favorable (Table. 1, carboxy-methano acetogenesis).

The LUCA era apparently proceeded in an environment with high CO₂ partial pressure, whereas the pre-LUCA period proceeded in a reducing environment with a significant availability of methane. The question thus arises: was this ancestral reverse acetyl-CoA relic pathway the only metabolic CH₄ fixation system, or were there other proto-biochemical mechanisms for the assimilation of carbon?

In addition to the acetyl-CoA pathway, autocatalytic CO₂ fixation cycles have been suggested as the first metabolic autocatalytic systems on early Earth (Wächtershäuser, 1990; Smith and Morowitz, 2004; Marakushev and Belonogova, 2009, 2013; Fuchs, 2011; Braakman and Smith, 2012, 2013). These include an autocatalytic reductive tricarboxylic acids (rTCA) cycle (reverse citrate cycle, Arnon cycle), a 3-hydroxypropionate cycle, a 3-hydroxypropionate/4-hydroxybutyrate cycle, a reductive dicarboxylate/4-hydroxybutyrate cycle, and a reducing pentose phosphate (Calvin–Benson–Bassham) cycle. The defined conservative sequences of intermediates of these cycles are modules such that their combination can create a variety of metabolic systems, including the specific pathways of carbon fixation (Lorenz et al., 2011; Marakushev and Belonogova, 2010, 2015; Braakman and Smith, 2012, 2013). To be considered a possible metabolic alternative, assimilating methane

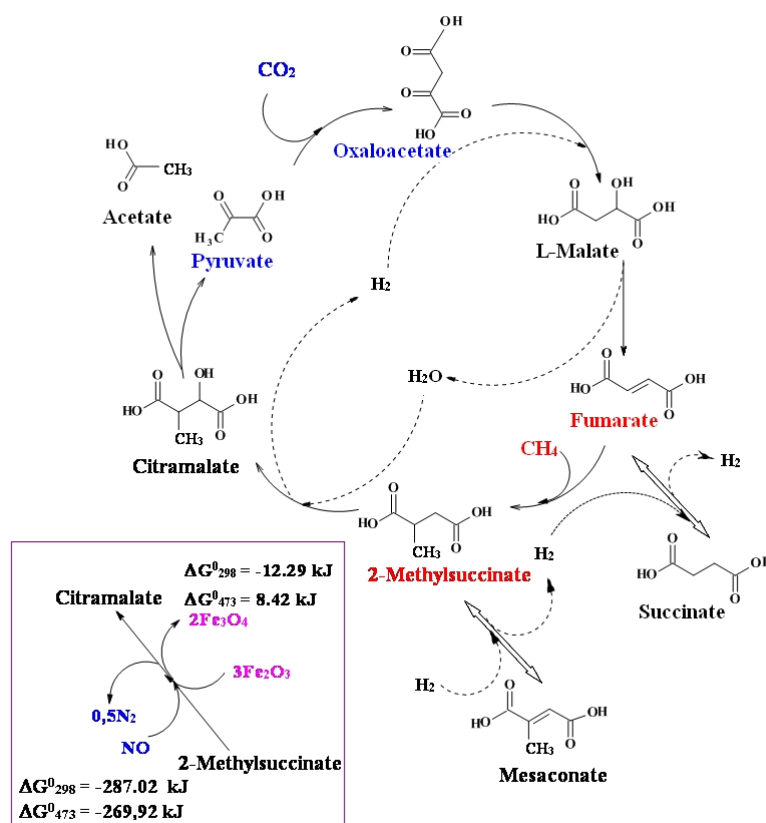
225 through autocatalytic cycle intermediates must satisfy the fundamental requirements of thermodynamics.

3 The proposed methane-fumarate cycle

230 Based on the hypothesis of primordial anaerobic methanotrophic metabolism origin, we assume that some components and modules of the metabolic cycles (carboxylic and keto acids, and their associations (parageneses)) may also be relicts of ancient methanotrophic metabolism. One of the few known reactions of CH₄ fixation is the formation of 2-methylsuccinate as a result of the reaction: fumarate+CH₄ → 2-methylsuccinate (Thauer and
235 Shima, 2008; Haynes and Gonzalez, 2014). Regeneration of fumarate can occur in various metabolic cycles, for example, fumarate+CH₄ → 2-methylsuccinate → mesaconate+2H → citramalate → citramalyl-CoA → pyruvate+acetyl-CoA →→→ oxaloacetate → citrate → isocitrate → 2-oxoglutarate+CO₂+2H → succinyl-CoA+CO₂+2H → succinate → fumarate+2H or fumarate+CH₄ → 2-methylsuccinate → 2-methylsuccinyl-CoA → 2-
240 ethylmalonyl-CoA → butyryl-CoA+CO₂ → crotonyl-CoA+2H → 3-hydroxybutyryl-CoA → 4-hydroxybutyryl-CoA → 4-hydroxybutyrate → succinate semialdehyde+2H → succinyl-CoA+2H →succinate → fumarate+2H (Thauer and Shima, 2008).

Fumarate addition has been widely proposed as an initial step in the anaerobic oxidation of both aromatic and aliphatic hydrocarbons (Musat, 2015). The reaction of methane with
245 fumarate satisfies the “minimal energy requirements” for autotrophic growth (Beasley and Nanny, 2012), and we consider the possibility of its participation in nascent autotrophic metabolism. We propose a simplified model of the methane-fumarate (MF) cycle, Fig. 2, which could have originated in the reductive Archean hydrothermal systems, at a high partial pressure of endogenous methane (facies II, Figure 1). Cycle is initiated by the reaction of
250 fumarate + methane → 2-methylsuccinate. In the hydration and dehydrogenation or anaerobic oxidation reactions, 2-methylsuccinate is converted to citramalate, which is disproportionated to acetate and pyruvate with cleavage of carbon-carbon bond. Pyruvate is an important “hub” metabolite that is a precursor for amino acids, carbohydrates, cofactors, and lipids in extant metabolic network. The following carbon assimilation reaction in the form of CO₂ with the
255 formation of oxaloacetate is a biomimetic analogue of the reductive tricarboxylic acid (rTCA) cycle reaction. An α-carboxylation of pyruvate is a critical anabolic pathway in modern biochemistry, which resupplies rTCA cycle intermediates. Oxaloacetate is transformed into fumarate in the reactions of the citrate cycle intermediates. The resulting fumarate assimilates

methane and begins a new MF cycle, in one turnover of which an acetate molecule is formed
 260 from methane and carbon dioxide molecules: $\text{CH}_4 + \text{CO}_2 = \text{CH}_3\text{COOH}$, Table. 1. The
 nonenzymatic flow of some reaction sequences of the rTCA cycle, such as oxaloacetate \rightarrow
 malate \rightarrow fumarate \rightarrow succinate has been recently experimentally confirmed (Muchowska et
 al., 2017).



265 **Figure 2.** The scheme of the proposed methane-fumarate (MF) cycle. Carbon from methane
 is introduced into the fumarate (marked by red), and from CO₂ into the pyruvate (marked by
 blue) with the formation of a C–C bond. The reaction sequence pyruvate \rightarrow oxaloacetate \rightarrow
 malate \rightarrow fumarate \rightarrow succinate is part of the reductive tricarboxylic acid (rTCA) cycle an
 enzyme-free archaic version of which is proposed as the basis of ancient autotrophic
 270 metabolism (Wächtershäuser 1990; Smith and Morowitz 2004). The inset shows options for
 the oxidative transformation of 2-methylsuccinate to citramalate with hematite (Fe₂O₃) and
 nitric oxide (NO) as oxidants. The chemical potential of hydrogen in the environment
 determines the equilibrium shift in the reactions succinate \leftrightarrow fumarate and 2-methyl succinate
 \leftrightarrow mesaconate.

275

Transformation of fumarate into 2-methylsuccinate introduces into the cycle five-carbon intermediates, such as citramalate and mesaconate, functioning, for example, in the reductive 3-hydroxypropionate CO₂ fixation cycle. The autocatalytic nature of the cycle derives from the branching point associated with citramalate cleavage, and can be shown by the example of doubling the intermediate as in the reaction: C₄H₆O₅ (malate) + 1,5CH₄+2,5CO₂ = 2C₄H₆O₅ (two malate). This type of autotrophic metabolism, as in the case of the acetyl-CoA pathway, can be defined as carboxy-methanotrophic acetogenesis. The problem of the most energetically unfavorable reaction of 2-methylsuccinate transformation into citramalate ($\Delta G^0_{298} = 96.57$ kJ), Table 2a, can be solved by using oxidants, such as oxides of nitrogen and iron (Fig. 2, inset). Nitric oxide (NO) is the strongest oxidant, but the reaction with Fe₂O₃ is also favorable at physiological temperatures.

Table 2. The free energy of reactions of MF cycle (a) and reactions of its anaerobic oxidative branch (b) with different oxidants at 298 and 473 K and P_{SAT}. TR – represents the temperature regime of the reactions. For comparison, the reactions of methane oxidation with molecular oxygen are considered. Free energies of aqueous substances formation at P_{SAT} (Amend and Shock, 2001; Marakushev and Belonogova, 2012, 2013 (El. Suppl. Mat.)) were used in calculations.

a. Reactions of cycle	ΔG^0_{298} kJ/mol	ΔG^0_{473} kJ/mol	TR
1. (CH ₂) ₂ (COOH) ₂ (fumarate) + CH ₄ = (CH ₂)(CH ₃ CH)(COOH) ₂ (2-methylsuccinate)	-44.95	-29.97	L
2. (CH ₂)(CH ₃ CH)(COOH) ₂ + H ₂ O = (CH ₃ CH)CH(OH)(COOH) ₂ (citramalate) + H ₂	96.57	94.14	H
3. (CH ₃ CH)CH(OH)(COOH) ₂ = CH ₃ COOH (acetate) + CH ₃ (CO)COOH (pyruvate)	19.35	1.73	H
4. CH ₃ (CO)COOH + CO ₂ = CH ₂ CO(COOH) ₂ (oxaloacetate)	13.11	35.03	L
5. CH ₂ CO(COOH) ₂ + H ₂ = CH ₂ CH(OH)(COOH) ₂ (malate)	-65.49	-55.78	L
6. CH ₂ CH(OH)(COOH) ₂ = (CH ₂) ₂ (COOH) ₂ + H ₂ O	5.68	-5.26	H
7. (CH ₂) ₂ (COOH) ₂ (fumarate) + H ₂ = (CH ₂) ₂ (COOH) ₂ (succinate)	-102.24	-88.88	L
8. (CH ₃ C=CH)(COOH) ₂ (mesaconate) + H ₂ = (CH ₂)(CH ₃ CH)(COOH) ₂	-66.53	-54.85	L
b. Oxidative reactions of cycle methane branch	ΔG^0_{298} kJ/mol	ΔG^0_{473} kJ/mol	TR
(CH ₂) ₂ (COOH) ₂ (fumarate) + CH ₄ + H ₂ O = CH ₃ COOH (acetate) + CH ₃ (CO)COOH (pyruvate) + H ₂	70.97	65.9	H
(CH ₂) ₂ (COOH) ₂ + CH ₄ + 0.5O ₂ = CH ₃ COOH + CH ₃ (CO)COOH	-192.22	-182.53	L
(CH ₂) ₂ (COOH) ₂ + CH ₄ + Fe ₃ O ₄ + 1.5SiO ₂ = CH ₃ COOH + CH ₃ (CO)COOH + 1.5Fe ₂ SiO ₄	45.08	25.21	H
(CH ₂) ₂ (COOH) ₂ + CH ₄ + 3Fe ₂ O ₃ = CH ₃ COOH + CH ₃ (CO)COOH + 2Fe ₃ O ₄	22.38	13.87	H
(CH ₂) ₂ (COOH) ₂ + CH ₄ + 0.75FeS ₂ + 0.25Fe ₃ O ₄ = CH ₃ COOH + CH ₃ (CO)COOH + 1.5FeS	38.78	31.54	H

$(\text{CH}_2(\text{COOH})_2 + \text{CH}_4 + 2\text{HNO}_2 = \text{CH}_3\text{COOH} + \text{CH}_3(\text{CO})\text{COOH} + \text{H}_2\text{O} + 2\text{NO}$	-115.77	-143.28	H
$(\text{CH}_2(\text{COOH})_2 + \text{CH}_4 + 2\text{NO} = \text{CH}_3\text{COOH} + \text{CH}_3(\text{CO})\text{COOH} + \text{N}_2\text{O}$	-274.7	-250.83	L
$(\text{CH}_2(\text{COOH})_2 + \text{CH}_4 + \text{NO} = \text{CH}_3\text{COOH} + \text{CH}_3(\text{CO})\text{COOH} + 0.5\text{N}_2$	-276.93	-264.48	L

295 The reversibility of the reactions in the citrate cycle is mainly determined by the equilibrium of fumarate+H₂ = succinate ($\Delta G^0_{298} = -102.24$, $\Delta G^0_{473} = -88.88$ kJ/mol), Table 2a. The change in the direction of electron flow therein is determined by the chemical potential of hydrogen (Marakushev and Belonogova, 2009), and therefore, different proto-metabolic cycles could be formed, for example, the oxidative citrate and reductive 3-hydroxipropionate
300 cycles (succinate → fumarate), the rTCA cycle (fumarate → succinate), or the proposed CH₄ fixation cycle (succinate → fumarate → 2-methylsuccinate).

Anaerobic methane oxidizing branch of cycle represents the transformation of fumarate to pyruvate and acetate. The free energies of these reactions with various inorganic oxidizing agents at 298 and 473 K are given in Table 2b. Assimilation of CH₄ in the oxidizing branch of
305 cycle, Fig. 2a, demonstrates highly favorable thermodynamics with all redox pairs of nitrogen. The same reaction with the iron redox pair becomes more favorable at temperature increasing. Reactions with iron mineral buffers, Table 2a, are closer to the equilibrium state, which ultimately determines the possibilities of primordial cycle flow in the forward or reverse directions (development of methanogenesis or methanotrophic acetogenesis). An
310 analysis of the oldest known association of microfossils suggests that methane-cycling methanogen-methanotroph communities were a significant component of Earth's early biosphere (Schopf et al., 2017). It is possible that a high methane partial pressure existed in a geodynamic regime of high endogenous methane flow in ancient Earth promoted formation of various versions of carbon assimilating systems.

315 Methyl group formation by the oxidation of methane is limited by kinetics, because the dissociation energy of the C–H bond in methane (439 kJ/mol) exceeds that of the X–H bond in other organic molecules, with the exception of the O–H bond in H₂O (497 kJ/mol) and other oxygen-derived molecular species. In the field of alkane oxidation, enzymatic metal-oxo species, promote C–H activation through a metallo-radical pathway. This involves hydrogen
320 radical abstraction from the alkane by the oxo species, followed by rapid rebound of the radical species onto the metal hydroxo intermediate (Roudesly et al., 2017). The calculation of the potential energy surface showed the thermodynamic possibility of anaerobic oxidation of methane via fumarate addition, in a reaction catalyzed by the glycy radical (Beasley and Nanny, 2012). The reaction mechanism fumarate + CH₄ → 2-methylsuccinate, fig. 2, seems
325 to be similar to the radical mechanism of breaking the C–H bond with the formation of the C–

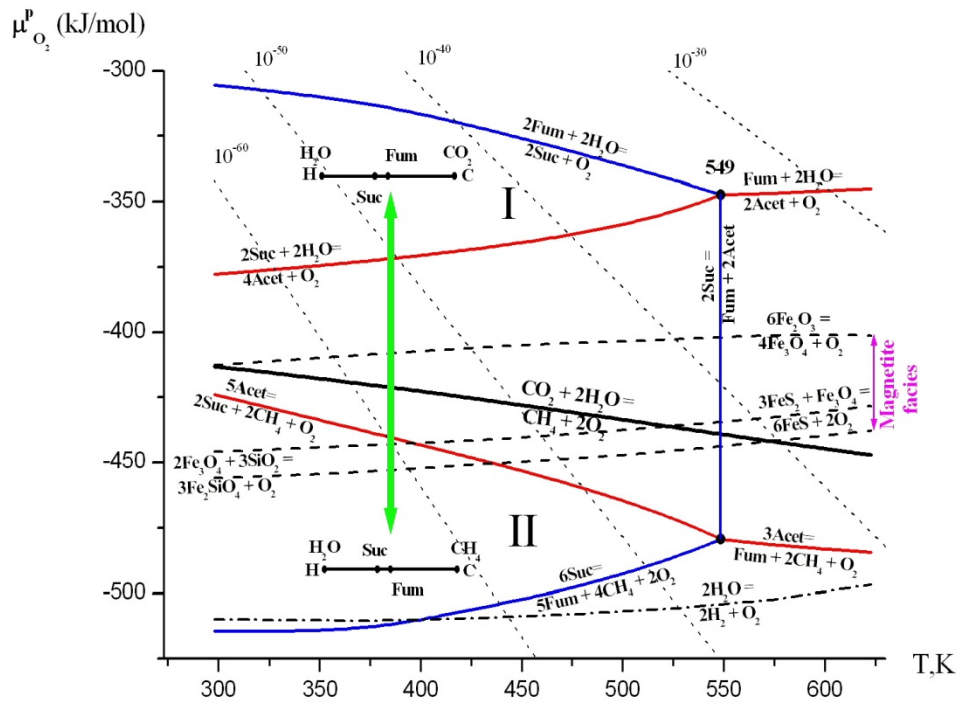
C bond, catalyzed by benzylsuccinate synthase (Buckel and Golding, 2006; Austin et al., 2011) during microbiological fixation of toluene by fumarate. Radicals of amino acids and dipeptides may be the possible catalysts of methane activation with the formation of methyl radical as an attacking agent. According to (Weiss et al., 2016), LUCA metabolism had an excess of radical reaction mechanisms, which, in our opinion, could also participate in the reaction of CH₄ fixation in the cycle, overcoming the activation barriers of kinetically unfavorable reaction steps. Moreover, these limitations are surmount in conditions of high substrate concentration and in the presence of metalocatalysts similar to the active center of mononuclear and polynuclear non-heme iron and iron-nickel enzymes.

Our understanding of the emergence of methanotrophic metabolism is within the framework of the hydrothermal theory for the origin of life with all its advantages (continuous flow of energy and matter, the temperature gradient, great possibilities of homogeneous and heterogeneous metal catalysis). Before the occurrence of cellular structures, the primary autotrophic metabolism on the surface of minerals created the space of competing autocatalytic carbon fixation cycles. The accumulation of “biomass” probably led to the emergence of heterotrophic protometabolism and the creation of a certain matrix of the organo-mineral system in which a cascade of proto-biochemical redox reactions could occur, such as in the modern soils (Kéroual et al., 2016). Regardless of the specific mechanism of the functioning of the precellular autotrophic metabolism (“reductive surface pyrite world” (Wächtershäuser, 1988), “hydrothermal reactor” (Russell and Martin, 2004.), “organo-mineral matrix” (Kéroual et al., 2016), and others) its origin and development was subject to the laws of aqueous thermodynamics.

4 Anaerobic methane oxidation in the hydrothermal systems

We represent the hydrothermal system in the form of a phase diagram which displays the chemical potential of oxygen vs. temperature at saturated vapor pressure (P_{SAT}), where temperatures and pressures are below critical thresholds (647,3 K and 22,1 MPa) (Fig. 3). The chemical potentials (μ_i) of components representing its partial energy, the value μ_i is expressed through activity α_i or fugacity f_i as follows: $\mu_i = (\mu_i^0)_{T,p} + RT \ln \alpha_i = (\mu_i^0)_{T,p} + RT \ln f_i$. Here numerical values depend on conventional standard states. For activity, the state of pure crystalline substance or unit molal concentration is usually considered as a standard state at given temperature and pressure. In this state $\alpha_i = 1$ and, hence, $\mu_i = (\mu_i^0)_{T,p}$. The diagram is a two-component system (extensive parameters: C and H), since oxygen become intensive

360 parameters, as the temperature, and pressure. Oxygen is represented by the chemical potential of O₂ in hydrothermal solution ($\mu^P_{O_2} = RT \ln a_{O_2}$, where a_{O_2} denotes the chemical activity of oxygen). According to the Gibbs' phase rule, at arbitrary pressure, the nonvariant equilibria in the diagram (points) consist of four phases, and the three-phase equilibria (lines) divide the divariant stability fields (facies) of the two-phase equilibria.



365 **Figure 3.** Diagram of the chemical potential of oxygen ($\mu^P_{O_2}$) - temperature (T, K) at saturated vapor pressure (P_{SAT}). The areas of thermodynamic stability of substances and their parageneses were calculated according to the method described in Korzhinskii, 1959 and Marakushev & Belonogova (2009). Points (indicated by temperature values) and lines represent four-phase and three-phase equilibria, separating the two-phase divariant fields of substance stabilities. The bold black line represents the equilibrium of $CO_2 \leftrightarrow CH_4$ and separates their areas of thermodynamic stability (I and II). The dashed lines are equilibria of mineral buffers: hematite-magnetite, Fe_2O_3/Fe_3O_4 (HM), pyrite-pyrrhotite-magnetite, $FeS_2+Fe_3O_4/FeS$ (PPM), and quartz-magnetite-fayalite, $SiO_2+Fe_3O_4/Fe_2SiO_4$ (QMF). The isolines of the activity of O₂ (10^{-n} M, dot lines) are drawn. The acetate and succinate facies contoured with red and blue equilibria, respectively. We provide only two linear diagrams of the two-component C-H system in the CO₂ and CH₄ facies. The transition between this facies with the change of oxygen chemical potential of is indicated by a green arrow. Abbreviation: Succinate – Suc, Fumarate – Fum, Acetate –Acet.

370

375

The equilibrium $\text{CH}_4 + 2\text{O}_2 = \text{CO}_2 + 2\text{H}_2\text{O}$ (bold black line) divides the diagram into the facies of CO_2 (**I**) and CH_4 (**II**) (oxic and anoxic areas of the hydrothermal system) and illustrates the two main possibilities for the development of the C–H–O system in the facies carbon dioxide or methane. Intermediates of the MF cycle are acetate, succinate, and fumarate, and we considered their metastable equilibria and parageneses. In all phase space under consideration, there are fumarate facies. The equilibrium of $5\text{Fum} + 4\text{CH}_4 + 2\text{O}_2 = 6\text{Suc}$ at low-temperature (Fig. 3), is located in the region of very low partial pressures of oxygen, whereas the equilibrium of $\text{Fum} + 2\text{CH}_4 + \text{O}_2 = 3\text{Acet}$ at high-temperature occurs in facies of high pressures. Acetate and succinate facies (contoured with red and blue equilibria, respectively) completely encompass the equilibrium of $\text{CH}_4 + \text{O}_2 = \text{CO}_2 + \text{H}_2\text{O}$. That is, in hydrothermal solution, the parageneses of some components within the MF cycle are stable in both the CO_2 and the CH_4 facies. The whole system can develop in either of two directions as the chemical potential of oxygen changes: 1. the formation of low-temperature (Suc- H_2O) and high-temperature (Fum- H_2O) paragenesis in CO_2 facies (**I**) and 2. the formation of low-temperature (Suc- CH_4) and high-temperature (Fum- CH_4) paragenesis in CH_4 facies (**II**). Thus, within these facies, protobiochemical systems supporting carbon fixation in the form of CO_2 or CH_4 can develop, and methane facies (**II**) represent a broad area of CH_4 assimilation by carboxylic acids in an aqueous environment. The high stability of the succinate-fumarate-acetate paragenesis in hydrothermal systems at 200°C (473 K) was experimentally shown (Estrada et al., 2017).

Mineral buffers up to 549 K are located in the facies of succinate, but the equilibrium of HM remains in the area of thermodynamic CO_2 stability (facies **I**), and PPM and QMF equilibria occur in methane facies **II** and intersect the fundamental equilibrium of $2\text{Suc} + 2\text{CH}_4 + \text{O}_2 = 5\text{Acet}$. Magnetite (Fe_3O_4) facies (between HM and QMF equilibria) encompass CH_4/CO_2 equilibrium in nearly the entire temperature range of the hydrothermal system under consideration. Thus, the redox areas of magnetite stability correspond to the formation conditions both CO_2 and CH_4 assimilating systems. The presence of magnetite in the early Archean ocean was shown by (Li et al., 2017]. Shibuya et al. (2016) also conclude that iron redox reactions probably played important role in the early evolution of methanotrophic metabolisms in the Hadean alkaline hydrothermal system. The QMF buffer equilibrium is completely located in the methane facies (**I**), which, according to data (Yang et al., 2014), corresponds on average to the redox conditions of Hadean mantle and crust. Up to the 3.6 billion years ago and maybe even to the great oxidative event of 2.2-2.4 billion years

ago on, the Earth's surface the oxidation potential of the magnetite redox pairs, apparently,
415 determined the chemical potential of environmental oxygen.

5 Conclusion

The cyclic planetary fluid flows (outgassing of volatiles from mantle) drive Earth's
420 chemical evolution, leading to the formation of different geobiochemical systems of carbon
fixation. Impulses of CO₂ and CH₄ degassing on our planet must have determined the
preference of specific autotrophic carbon fixation metabolism development. It is generally
accepted that autotrophic metabolism is the fixation of inorganic carbon solely in the form of
CO₂, but CH₄ is also deep and inorganic; therefore, carbon fixation from methane is also a
425 manifestation of autotrophic metabolism. The variety of modern autotrophic carbon fixation
seems to be created by the association of the different metabolic associations and modules
that, apparently, could function in the ancestral systems of the anaerobic fixation of CH₄.
When a CO₂ degassing regime began to dominate on our planet, relict systems of
methanotrophy were forced to die out or to be thrown back into uncommon and extreme
430 ecological niches. If we consider LUCA as a relatively recent player in the evolution of life
(Cornish-Bowden and Cárdenas, 2017), the ancestral metabolic systems of carbon fixation in
putative pre-LUCA could differ appreciably from modern ones.

In the process of development of CO₂ fixation systems on Earth, the main problem was
the presence of electron donors (therefore, evolution created selective reducing agents:
435 NADH, NADPH, FADH), whereas the fixation of CH₄ essentially depended on the presence
of electron acceptors. In the hydrothermal systems, oxygen-containing nitrogen compounds
are the best oxidants, but we believe that the redox pairs of hematite-magnetite and quartz-
magnetite-fayalite create a specific area of chemical potential of oxygen that satisfies the
thermodynamic requirements of oxidation and assimilation of methane by protometabolic
440 pathways. Hydrothermal systems of ancient Earth may have been very similar to those that
currently exist on some extraterrestrial cosmic bodies, such as Europa or Enceladus. The
degassing of these cosmic bodies can currently support methane metabolism, but the problem
is to know if there are electron acceptors there (Russell et al., 2017).

445 Author Disclosure Statement

No competing financial interests exist.

References

- 450 Alldredge, L.R.: A discussion of impulses and jerks in the geomagnetic field, *J. Geophys. Res.*, 89, 4403–4412, doi: 10.1029/JB089iB06p04403, 1984.
- Amend, J.P., and Shock, E.L.: Energetics of overall metabolic reactions of thermophilic and hyperthermophilic Archaea and Bacteria, *FEMS Microbiol. Rev.*, 25, 175–243, doi: 10.1016/S0168-6445(00)00062-0, 2001.
- 455 Aubert, J., Tarduno, J.A., and Johnson, C.L.: Observations and models of the long-term evolution of earth's magnetic field, *Space Sci. Rev.*, 155, 337–370, doi: 10.1007/s11214-010-9684-5, 2010.
- Aulbach, S., Woodland, A. B., Vasilyev, P., Galvez, M. E. and Viljoen K. S.: Effects of low-pressure igneous processes and subduction on $\text{Fe}^{3+}/\text{ZFe}$ and redox state of mantle eclogites from Lace (Kaalvaal craton), *Earth Planet. Sci. Lett.*, 474, 283–295, 2017.
- 460 Austin, R.N., and Groves, J.T.: Alkane-oxidizing metallo enzymes in the carbon cycle, *Metallomics*, 3, 775–787, doi: 10.1039/c1mt00048a, 2011.
- Beal, E.J., House, C.H., and Orphan, V.J.: Manganese- and iron-dependent marine methane oxidation, *Science*, 325, 184–187, doi: 10.1126/science.1169984, 2009.
- 465 **Beasley, K.K., and Nanny M.A.: Potential energy surface for anaerobic oxidation of methane via fumarate addition, *Environ. Sci. Technol.*, 46, 8244–8252, doi: 10.1021/es3009503, 2012.**
- Boehnke, P., Bell, E.A., Stephana, T., Trappitscha, R., Keller, C. B., Pardo, O.S., Davis, A.M., Harrisonc, T. M. and Pellina, M.: Potassic, high-silica Hadean crust, *Proc. Natl. Acad. Sci.* 115, 6353-6356, doi: 10.1073/pnas.1720880115, 2018.**
- 470 Bouquet, A., Mousis, O., Waite, J.H., and Picaud, S.: Possible evidence for a methane source in Enceladus' ocean, *Geophys. Res. Lett.*, 42, 1334–1339, doi: 10.1002/2014GL063013, 2015.
- Braakman, R., and Smith, E.: The emergence and early evolution of biological carbon-fixation, *PLOS Comput. Biol.*, 8, 1–16, doi: 10.1371/journal.pcbi.1002455, 2012.
- 475 Braakman, R., and Smith, E.: The compositional and evolutionary logic of metabolism, *Phys. Biol.*, 10, 1–63, doi: 10.1088/1478-3975/10/1/011001, 2013.
- Brovarone, A.V., Martinez I., Elmaleh A., Compagnoni R., Chaduteau C., Ferraris C., and Esteve I.: Massive production of abiotic methane during subduction evidenced in metamorphosed ophicarbonates from the Italian Alps, *Nat. Commun.*, 8, 14134, doi: 10.1038/ncomms14134, 2017.**
- 480

Buckel, W., and Golding, B.T.: Radical enzymes in anaerobes, *Ann. Rev. Microbiol.*, 60, 27-49, doi: 10.1146/annurev.micro.60.080805.142216, 2006.

485 Cornish-Bowden, A., and Cárdenas, M.L.: "Life Before LUCA," *J. Theor. Biol.*, 434, 68–74, doi: 10.1016/j.jtbi.2017.05.023, 2017.

Estrada, C.F., Mamajanov, I., Hao, J., Sverjensky, D.A., Cody, G.D., and Hazen, R.M.: Aspartate transformation at 200 °C with brucite [Mg(OH)₂], NH₃, and H₂: implications for prebiotic molecules in hydrothermal systems, *Chem. Geol.*, 457, 162–172, doi: 10.1016/j.chemgeo.2017.03.025, 2017.

490 Ettwig, K.F., Butler, M.K., Le Paslier, D., Pelletier, E., Mangenot, S., Kuypers, M.M., Schreiber, F., Dutilh, B.E., Zedelius, J., de Beer, D., Gloerich, J., Wessels HJ, van Alen T, Luesken F, Wu ML, van de Pas-Schoonen KT, Op den Camp HJ, Janssen-Megens, E.M., Francoijs, K.J., Stunnenberg, H., Weissenbach, J., Jetten, M.S., and Strous, M.: Nitrite-driven anaerobic methane oxidation by oxygenic bacteria, *Nature*, 464, 543–548, doi: 10.1038/nature08883, 2010.

495 Ettwig, K.F., Zhu, B., Speth, D., Keltjens, J.T., Jetten, M.S.M., and Kartal, B.: Archaea catalyze iron-dependent anaerobic oxidation of methane, *Proc. Natl. Acad. Sci.*, 113, 12792–12796, doi: 10.1073/pnas.1609534113, 2016.

Fuchs, G.: Alternative pathways of carbon dioxide fixation: Insights into the early evolution of life? *Ann. Rev. Microbiol.*, 65, 631–658, doi: 10.1146/annurev-micro-090110-102801, 2011.

Haroon, M.F., Hu, S., Shi, Y., Imelfort, M., Keller, J., Hugenholtz, P., Yuan, Z., and Tyson, G.W.: Anaerobic oxidation of methane coupled to nitrate reduction in a novel archaeal lineage, *Nature*, 500, 567–570. DOI: 10.1038/nature12375, 2013.

505 Haynes, C.A., and Gonzalez, R.: Rethinking biological activation of methane and conversion to liquid fuels, *Nature Chem. Biol.*, 10, 331–339, doi: 10.1038/nchembio.1509, 2014.

He, Z., Zhang, Q., Feng, Y., Luo, H., Pan, X., and Gadd, G.M.: Microbiological and environmental significance of metal-dependent anaerobic oxidation of methane, *Sci. Total Environ.*, 610–611, 759–768, doi: 10.1016/j.scitotenv.2017.08.140, 510 2018.

Hinrichs, K.U., Hayes, J.M., Sylva, S.P., Brewer, P.G., and DeLong, E.F.: Methane-consuming archaeobacteria in marine sediments, *Nature*, 398, 802–805. doi :10.1016/S0146-6380(00)00106-6, 1999.

Kéroual, B., Lehours, A.C., Colombet, J., Amblard, C., Alvarez, G. and Fontaine, S.: Soil carbon dioxide emissions controlled by an extracellular oxidative metabolism

515

identifiable by its isotope signature, *Biogeosciences* 13, 6353–6362, doi:10.5194/bg-13-6353-2016, 2016.

Knittel, K., and Boetius, A.: Anaerobic oxidation of methane: progress with an unknown process. *Ann. Rev. Microbiol.*, 63, 311–334, doi: 10.1146/annurev.micro.61.080706.093130, 2009.

Korzhinskii, D.S.: *Physicochemical basis of the analysis of the paragenesis of minerals*, Consultants Bureau, Inc. (New York), and Chapman & Hall (London), 1959.

Larson, R.L., and Olson, P.: Mantle plumes control magnetic reversal frequency, *Earth Planet. Sci. Lett.*, 107, 437–447, doi: 10.1016/0012-821X(91)90091-U, 1991.

Li, Yi-L., Konhauser, K.O. and Zhai, M.: The formation of magnetite in the early Archean oceans, *Earth Planet. Sci. Lett.*, 466, 103–114, doi: 10.1016/j.epsl.2017.03.013, 2017.

Lorenz, D.M., Jeng, A., and Deem, M.W.: The emergence of modularity in biological systems, *Phys. Life Rev.*, 8, 129–160, doi: 10.1016/j.plrev.2011.02.003, 2011.

Marakushev, A.A., and Marakushev, S.A.: PT facies of elementary, hydrocarbon, and organic substances, *Dokl. Earth Sci.*, 406, 141–147, doi: 10.1134/S1028334X0601034X, 2006.

Marakushev, A.A., and Marakushev, S.A.: Formation of oil and gas fields, *Lithol. Miner. Resour.*, 43, 454–469, doi: 10.1134/S0024490208050039, 2008.

Marakushev, A.A., and Marakushev, S.A.: Fluid evolution of the Earth and origin of the biosphere, in: *Man and the Geosphere*, edited by: Florinsky, I.V., Nova Science Publishers Inc, New York, 3–31, 2010.

Marakushev, S.A., and Belonogova, O.V.: The parageneses thermodynamic analysis of chemoautotrophic CO₂ fixation archaic cycle components, their stability and self-organization in hydrothermal systems, *J. Theor. Biol.*, 257, 588–597, doi: 10.1016/j.jtbi.2008.11.032, 2009.

Marakushev, S.A., and Belonogova, O.V.: Metabolic design and biomimetic catalysis of the archaic chemoautotrophic CO₂ fixation cycle, *Mos. Univer. Chem. Bull.*, 65, 212–218, doi: 10.3103/S0027131410030211, 2010.

Marakushev, S.A., and Belonogova, O.V.: Thermodynamic factors of natural selection in autocatalytic chemical systems, *Dokl. Biochem. Biophys.*, 444, 131–136, doi: 10.1134/S1607672912030015, 2012.

Marakushev, S.A., and Belonogova, O.V.: The divergence and natural selection of autocatalytic primordial metabolic systems, *Orig. Life Evol. Biosph.*, 43, 263–281, doi: 10.1007/s11084-013-9340-7, 2013.

- Marakushev, S.A., and Belonogova, O.V.: The Chemical Potentials of Hydrothermal Systems
550 and the Formation of Coupled Modular Metabolic Pathways, *Biophysics*, 60, 542–552,
doi: 10.1134/S0006350915040168, 2015.
- Martin, W.F., Weiss, M.C., Neukirchen, S., Nelson-Sathi, S., and Sousa, F.L.: Physiology,
phylogeny, and LUCA, *Microbial Cell*, 3, 582–587, doi: 10.15698/mic2016.12.545,
2016.
- 555 Martinez-Cruz, K., Leewis, M.-C., Herriott, I.C., Sepulveda-Jauregui, A., Anthony, K.W.,
Thalasso, F., and Leigh, M.B.: Anaerobic oxidation of methane by aerobic
methanotrophs in sub-Arctic lake sediments, *Sci. Total Environ.*, 607–608, 23–31, doi:
10.1016/j.scitotenv.2017.06.187, 2017.
- Mével, C.: Serpentinization of abyssal peridotites at mid-ocean ridges, *C. R. Geosci.*, 335,
560 825–852, doi: 10.1016/j.crte.2003.08.006, 2003.
- Muchowska, K. B., Varma, S.J., Chevallot-Beroux, E., Lethuillier-Karl, L., Li G., and Moran,
J.: Metals promote sequences of the reverse Krebs cycle, *Nat. Ecol. Evol.*, 1, 1716–
1721, doi: 10.1038/s41559-017-0311-7, 2017.
- Musat, F.: The anaerobic degradation of gaseous, nonmethane alkanes - From in situ
565 processes to microorganisms, *Comput. Struct. Biotechn. J.*, 13 222–228, doi:
10.1016/j.csbj.2015.03.002, 2015.
- Nitschke, W., and Russell, M.J.: Beating the acetyl-CoA pathway to the origin of life, *Phil.*
Trans. Royal Soc. London, Series B, 368, 20120258, doi: 10.1098/rstb.2012.0258,
2013.
- 570 Nivin, V.A., Treloar, P.J., Konopleva, N.G., and Ikorsky, S.V.: A review of the occurrence,
form and origin of C-bearing species in the Khibiny alkaline igneous complex, Kola
Peninsula, NW Russia, *Lithos*, 85, 93–112, doi: 10.1016/j.lithos.2005.03.021, 2005.
- Oehler, D.Z., and Etiope, G.: Methane seepage on Mars: where to look and why, *Astrobiol.*,
17, 1233–1264, doi: 10.1089/ast.2017.1657, 2017.
- 575 Oni, O.E. and Friedrich, M.W.: Metal oxide reduction linked to anaerobic methane oxidation,
Trends Microbiol., 25, 88–90, doi: 10.1016/j.tim.2016.12.001, 2017.
- Potter, J., and Konnerup-Madsen, J.: A review of the occurrence and origin of abiogenic
hydrocarbons in igneous rocks, in: *Hydrocarbons in Crystalline Rocks*, edited by:
Petford, N., and McCaffrey, K.J.W., Special Publications, 214, Geological Society,
580 London, 151–173, doi:10.1144/GSL.SP.2003.214.01.10, 2003.

- Roudesly, F., Oble, J., and Poli, G.: Metal-catalyzed C H activation/functionalization: The fundamentals, *J. Molec. Cat. A: Chem.*, 426, 275–296, doi: 10.1016/j.molcata.2016.06.020, 2017.
- Russell, M.J., and Martin, W.: The rocky roots of the acetyl-CoA pathway, *Trends Biochem. Sci.* 29, 358-363, doi: 10.1016/j.tibs.2004.05.007, 2004.
- 585 Russell, M.J., Murray, A.E., and Kevin, P.H.: The possible emergence of life and differentiation of a shallow biosphere on irradiated icy worlds: The example of Europa, *Astrobiol.*, 17, 1265–1273, doi: 10.1089/ast.2016.1600, 2017.
- Russell, M.J., and Nitschke, W.: Methane: Fuel or Exhaust at the Emergence of Life? *Astrobiol.*, 17, 1053–1066, doi: 10.1089/ast.2016.1599, 2017.
- 590 Schopf, J.W., Kitajima, K., Spicuzza M.J., Kudryavtsev A.B., and Valley, J.W.: SIMS analyses of the oldest known assemblage of microfossils document their taxon-correlated carbon isotope compositions, *Proc. Natl. Acad. Sci. USA*, 115, 53–58, doi: 10.1073/pnas.1718063115, 2017.
- 595 Scheller, S., Goenrich, M., Boecher, R., Thauer, R.K., and Jaun, B.: The key nickel enzyme of methanogenesis catalyses the anaerobic oxidation of methane, *Nature*, 465, 606–609, doi: 10.1038/nature09015, 2010.
- Schreiber, U., Mayer, C., Schmitz, O.J., Rosendahl, P., Bronja A, Greule, M., Keppler, F., I. Mulder, I., Sattler, T., and Schöler, H.F.: Organic compounds in fluid inclusions of Archean quartz–Analogues of prebiotic chemistry on early Earth, *PLoS ONE*, 12, e0177570, doi.org/10.1371/journal.pone.0177570, 2017.
- 600 Semrau, J.D., DiSpirito, A.A., and Murrell, J.C.: Life in the extreme: thermoacidophilic methanotrophy, *Trends Microbiol.*, 16, 190–193, doi: 10.1016/j.tim.2008.02.004, 2008.
- Shibuya, T., Russell, M.J., and Takai, K.: Free energy distribution and hydrothermal mineral precipitation in Hadean submarine alkaline vent systems: Importance of iron redox reactions under anoxic conditions, *Geochim. Cosmochim. Acta*, 175, 1–19, doi: 10.1016/j.gca.2015.11.021, 2016.
- 605 Smejkalová, H., Erb, T.J., and Fuchs, G.: Methanol assimilation in *Methylobacterium extorquens* AM1: demonstration of all enzymes and their regulation, *PLoS ONE*, 5, e13001, doi: 10.1371/journal.pone.0013001, 2010.
- 610 Smith, E. and Morowitz, H.G.: Universality in intermediary metabolism, *Proc. Natl. Acad. Sci. USA*, 101, 13168–13173, doi: 10.1073/pnas.0404922101, 2004.
- Smit, K.V., Shirey, S.B., Stern, R.A., Steele, A., and Wang, W.: Diamond growth from C–H–N–O recycled fluids in the lithosphere: Evidence from CH₄ micro-inclusions and δ¹³C–

- 615 $\delta^{15}\text{N-N}$ content in Marange mixed-habit diamonds, *Lithos*, 265, 68–81,
doi:10.1016/j.lithos.2016.03.015, 2016.
- Soo, V.W.C., McAnulty, M.J., Tripathi, A., Zhu, F., Zhang, L., Smith, P.B., Hatzakis, E.,
Agrawal, S., Nazem-Bokaei, H., Gopalakrishnan, S., Salis, H.S., Ferry, J.G., Maranas,
C.D., Patterson, A.D., and Wood, T.K.: Reversing methanogenesis to capture methane
620 for liquid biofuel precursors, *Microb. Cell Factories*, 15, 11–25, doi: 10.1186/s12934-
015-0397-z, 2016.
- Tao, R., Zhang, L., Tian, M., Zhu, J., Liu, X., Liu, J., Höfer, H.E., Stagno, V., and Fei, Y.:
Formation of abiotic hydrocarbon from reduction of carbonate in subduction zones:
Constraints from petrological observation and experimental simulation, *Geochim.*
625 *Cosmochim. Acta*, 239, 390–408, doi: 10.1016/j.gca.2018.08.008, 2018.
- Thauer, R.K., and Shima, S.: Methane as fuel for anaerobic microorganisms, *Ann. NY Acad.*
Sci., 1125, 158–170, doi: 10.1196/annals.1419.000.90, 2008.
- Tian, F., Toon, O. B., Pavlov, A. A. and De Sterck, H.: A hydrogen-rich early Earth
atmosphere, *Science*, 308, 1014–1017, 2005.
- 630 Tobie, G., Lunine, J.I., and Sotin, C.: Episodic outgassing as the origin of atmospheric
methane on Titan, *Nature*, 440, 61–64, doi: 10.1038/nature04497, 2006.
- Touret, J.L.R.: Remnants of early Archaean hydrothermal methane and brines in pillow-
breccia from the Isua-Greenstone Belt, West Greenland, *Precambrian Res.*, 126, 219–
233, doi: 10.1016/S0301-9268(03)00096-2, 2003.
- 635 Wachtershauser, G.: Before enzymes and templates: theory of surface metabolism, *Microbiol.*
Rev. 52, 452–484, doi:10.1101/cshperspect.a002162, 1988.
- Wächtershäuser, G.: Evolution of the first metabolic cycles, *Proc. Natl. Acad. Sci. USA*, 87,
200–204, doi: 10.1073/pnas.87.1.200, 1990.
- Wang, D.T., Reeves, E.P., McDermott, J.M., Seewald, J.S., and Ono, S.: Clumped
640 isotopologue constraints on the origin of methane at seafloor hot springs, *Geochim*
Cosmochim Acta, 223, 141–158, doi: 10.1016/j.gca.2017.11.030, 2018.
- Weiss, M.C., Sousa, F.L., Mrnjavac, N., Neukirchen, S., Roettger, M., Nelson-Sathi, S., and
Martin W.F.: The physiology and habitat of the last universal common ancestor, *Nature*
Microbiol., 1, 16116, doi: 10.1038/NMICROBIOL.2016.116, 2016.
- 645 Yang, X., Gaillard, F., and Scaillet, B.: A relatively reduced Hadean continental crust and
implications for the early atmosphere and crustal rheology, *Earth Planet. Sci. Lett.*, 393,
210–219, doi:10.1016/j.epsl.2014.02.056, 2014.

Zahnle, K.J., Gacesa, M. and Catling, D.C.: Strange messenger: A new history of hydrogen on Earth, as told by Xenon, *Geochim. Cosmochim. Acta* 244, 56–85, doi: [10.1016/j.gca.2018.09.017](https://doi.org/10.1016/j.gca.2018.09.017), 2019.